

A three-dimensional finite element analysis of two/multiple shots impacting on a metallic component

T. Hong[†]

College of Mechanical Engineering, Zhejiang University of Technology, Hangzhou, Zhejiang 310032, P.R. China

J.Y. Ooi

School of Engineering & Electronics, University of Edinburgh, King's Buildings, Edinburgh EH9 3JN, UK

B.A. Shaw

Department of Mechanical, Materials and Manufacturing Engineering, University of Newcastle, Newcastle upon Tyne NE1 7RU, UK

(Received July 5, 2007, Accepted June 20, 2008)

Abstract. This paper describes a three-dimensional dynamic finite element analysis of two/multiple shots impacting on a metallic component. The model is validated against a published numerical study. An extensive parametric study is conducted to investigate the effect of shot impacting with overlap on the resulting residual stress profile within the component, including time interval between shot impacts, separation distance between the impacting points, and impacting velocity of successive shots. Several meaningful conclusions can be drawn regarding the effect of shot impacting with overlap.

Keywords: shot peening; finite element analysis; residual stress; shot impacting with overlap.

1. Introduction

Many highly stressed engineering components such as railway axles, gears, crankshafts etc., which are often safety critical, are subjected to very many load cycles in their design life. In these cases, crack propagation is very rapid, and the time between crack initiation and total failure may only be minutes or hours of operation, and thus it is not practical to achieve high reliability by inspection or crack growth monitoring. In these cases, the only way of ensuring high structural integrity is to ensure that the fatigue strength of a component is greater than the fatigue stress. A very effective technique for improving component fatigue strength is the modification of near surface component stressing by shot peening. Shot peening is used in numerous engineering

[†] Ph.D., Corresponding author, E-mail: hz6770@hotmail.com

applications. It is a cold-work process in which a stream of tiny shots (0.2~2 mm) is blasted against an engineering component. Each shot impacts on the component surface, causing plastic deformation. After contact between the shot and the component ceased, a high compressive residual stress is generated at the surface layers of the component. Compressive residual stress in the surface layers of the component greatly improves the fatigue strength. It is therefore very useful to be able to predict the pattern and magnitude of the residual stress distribution near the surface after shot peening.

Shot peening is a very complex process to model numerically, involving dynamic analysis of fast moving shot impacting on a metallic component which can often have complex geometry. There are a significant number of parameters involved in shot peening which need to be controlled and regulated in order to produce a more beneficial compressive residual stress distribution within the component. These parameters can be categorised into three groups relating to the shot, the component and the process. The shot parameters include size, density, hardness, impact velocity, rotary inertia, oblique impact and so on. The component parameters include geometric and material properties such as initial yield stress, work hardening characteristics, hardness, strain-rate dependent and so on. The process parameters include mass flow rate, angle of attack, air pressure, distance between the nozzle and component, peening coverage and so on. In order to control the resulting residual stress pattern in peened components, it would be highly beneficial to establish quantitative relationships between these parameters and residual stress characteristics. Some progress has been made in recent years but the understanding of shot peening is still far from complete. The inter-relationships of the parameters and the residual stress characteristics are not clearly determined yet.

Study of the contact problem between elastic and elastic-plastic materials resulting from the loading of two bodies was pioneered by Hertz (1882). Further sources of references on indentation and allied subjects are given by Goldsmith (1960) and Johnson (1972). More recent analytical models (e.g., Al-Hassani 1981, Hills *et al.* 1983, Al-Obaid 1995) have been developed that predict the residual stress distribution and the plastically deformed region in single shot impacts on components. Because of the complexity of the shot peening process, simplifying assumptions were adopted. These assumptions make these analytic approaches unsuitable for dealing with practical applications with, for instance, complex geometry and non-linear material properties.

The Finite Element (FE) method provides a powerful tool for simulating shot impacting on a metallic component. The dynamic impacting of single or multiple shots with high velocity and the double non-linearity of the problem due to the contact of two bodies and the elastic-plastic behaviour of the component can all be taken into account in an appropriate FE analysis. Hardy *et al.* (1971) was the first to solve the contact problem of a rigid sphere indenting an elastic-perfect plastic half-space using the FE method. The first FE analysis of shot peening using the commercial FE program was presented by Edberg *et al.* (1995). They simulated a single shot impacting visco-plastic and elasto-plastic materials but the parameters used in their study do not represent realistic peening parameters. With the availability of greatly increased computing power and the widespread use of commercial FE programs in recent years, the use of FE analysis in simulating shot peening processes is becoming an increasingly attractive alternative (e.g., Schiffner and Helling 1999, Guagliano *et al.* 1999, Baragetti 2001). Al-Hassani *et al.* (1999) presented a numerical simulation of single and multiple shots impact on a component and examined single shot impacting with an oblique angle but very limited results were presented. Deslaef and Rouhaud (2000, 2002) presented a FE simulation of single and multiple shot impacting a component and examined the effect of rigid and deformable shot. The numerical results were compared with those experimental measurements

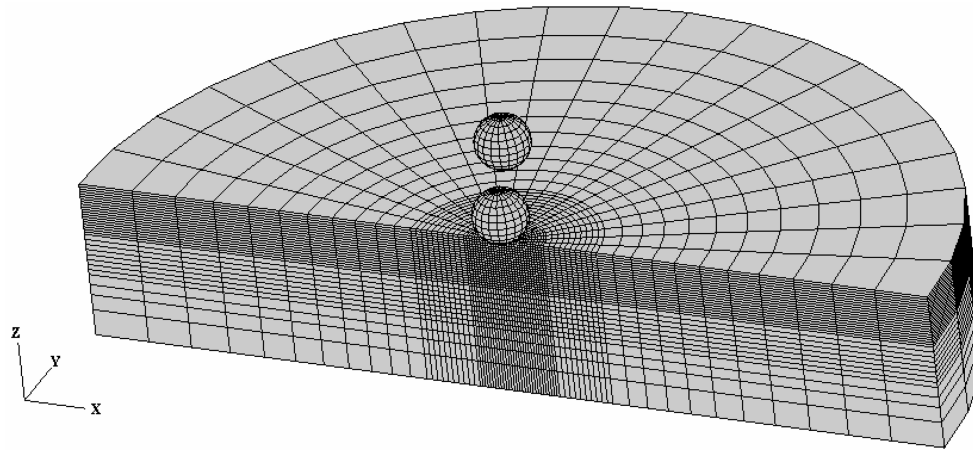
obtained for multiple shot impacts and showed significant differences. A more systematic study of shot peening using FE was presented by Meguid and his co-workers (1999, 2002). They conducted a dynamic FE analysis of single and multiple shot impacts. The effect of some parameters was investigated but not comprehensively.

In realistic shot peening process, most shots impact on a previously impacted area in which an existing residual stress distribution was induced by previous shot impacts. It is termed as shot impacting with overlap contact areas, simply as shot impacting with overlap. The previous numerical studies (e.g., Al-Hassani 1999, Deslaef and Rouhaud 2000, 2002, Meguid *et al.* 1999, 2002) have studied multiple shots impacting on a component. In most of these studies, the case of multiple shots impacting at the same time with non-overlap contact area was investigated. However, this scenario is far from realistic since, as a non-linear phenomenon, it can be expected that the sequence and separation of impact locations will affect the peening outcome. The behaviour of a shot impacting with overlap on a previously impacted area and the effect of successive overlap impacts is not well understood. The effect of successive shots impacting with overlap on the residual stress profile within a component does not appear to have been published before.

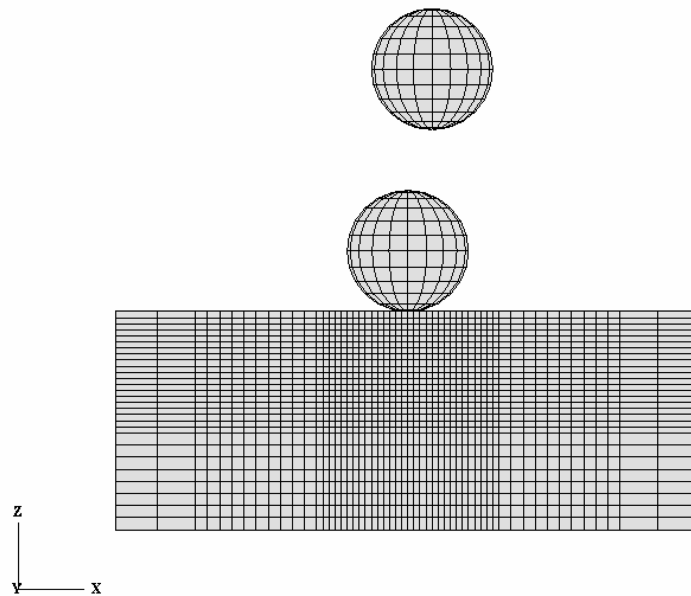
This paper describes a three-dimensional dynamic finite element (FE) analysis of two/multiple shots impacting on a metallic component. The prediction is validated by comparison with results from the published literature. An extensive parametric study is then performed with the aim of obtaining a better understanding of the behaviour of shot impacting with overlap and characterising the effect of successive overlap impacts on the resultant residual stress profile with a component including time interval between shot impacts, separation distance between the impacting points, and impacting velocity of successive shot. The relationships of these parameters and the resultant residual stress characteristics can then be extended to realistic multiple shot impacts.

2. Finite element model

The three-dimensional FE model was developed using the commercial finite element code ABAQUS 6.3 Explicit (2002). Figs. 1(a) and 1(b) show the FE model that was used to simulate two/multiple shots impacting on a component. Only one half of the circular plate was analysed by exploiting symmetry. The circular plate was restrained against all displacements and rotations on the bottom and was given the following geometric properties: radius $R = 8d_s$, height $H = 3d_s$ where d_s is the shot diameter. Nodal definitions are referred to a rectangular Cartesian coordinate system located at the centre of the circular plate, with the z -axis pointing in the upward direction and the x -axis and y -axis being on the top surface. Eight-node linear brick elements with reduced integration were used with element size $0.05d_s \times 0.05d_s \times 0.05d_s$ in the impact region. The kinematic formulation for these elements is to use the centroid strain formulation and the hourglass base vectors in the hourglass control. Shots chosen for industrial applications are often as hard as the impacted component material so for simplicity, a rigid sphere was chosen to model the shot. In ABAQUS, rigid bodies can be defined with an analytical rigid surface. So, a fully spherical surface with a mass positioned at its centre was used to model a shot as shown in Fig. 1. Convergence tests were conducted using different meshes and element types to ensure the numerical results were not affected by the choice of mesh or element types (Hong 2005).



(a) 3D model



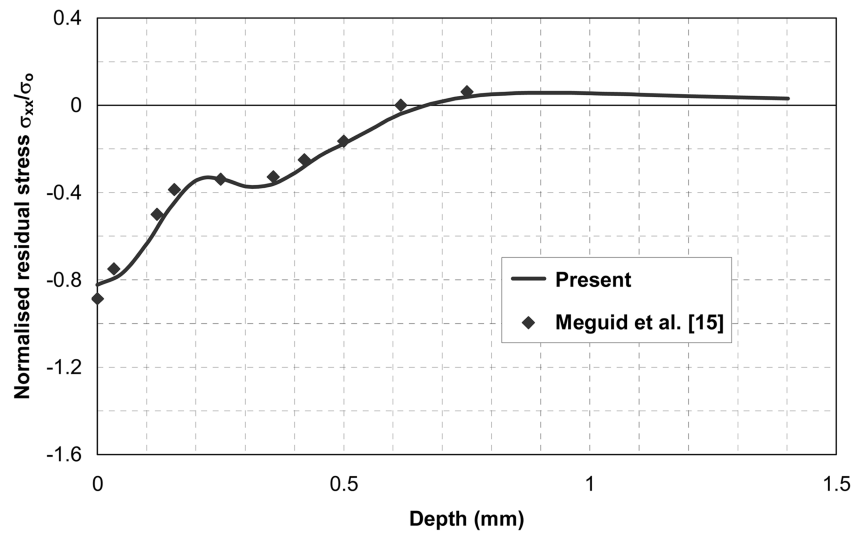
(b) Part of model (x-z plane)

Fig. 1 Three-dimensional FE model for two shots impacting on a component

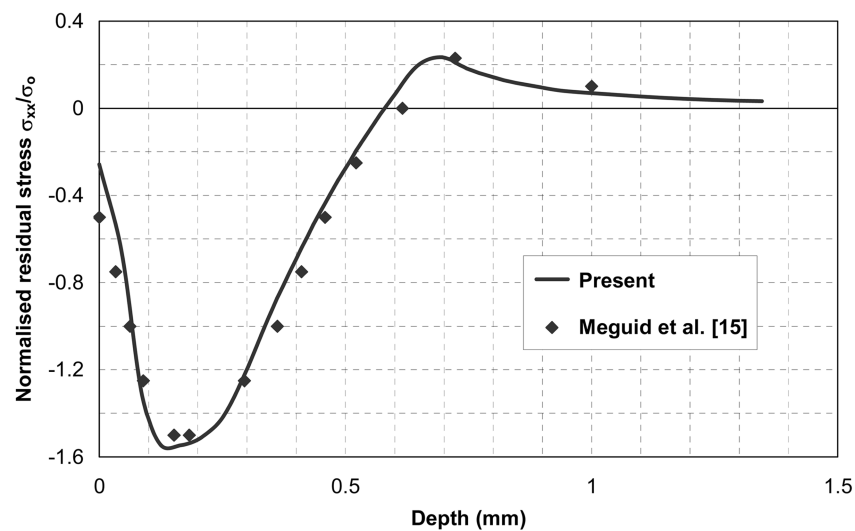
3. Numerical verification of two shots impact

Since no experimental measurement of two shots impacting on a component can be found in the published literature for comparison with this study, a comparison was made with the numerical study of Meguid *et al.* (1999) in which two shots impact normally on a metallic component at the same time with non-overlap contact areas. The geometric and material properties were used as following: width $W = 3.5$ mm, height $H = 2$ mm, breadth $B = 2.5$ mm, mass density $\rho = 7800$ kg/m³,

elastic modulus $E = 200$ GPa, initial yield stress $\sigma_o = 600$ MPa and a linear strain-hardening parameter $H^1 = 800$ MPa. The diameter and mass of identical shots was $d_s = 1$ mm and $m = 4.085$ mg respectively. The separation distance between the impacting points of these two shots is $2C = 1$ mm. Fig. 2(a) shows the variation of residual stress with depth along the central axis of the component for both Meguid *et al.* (1999) and the present study. The residual stress distribution with depth beneath the impacting point obtained by the present analysis is compared to those of Meguid *et al.* (1999) in Fig. 2(b). There is a close match between the two sets of numerical results, providing validation for the accuracy of the present analysis.



(a) Normalised residual stress σ_{xx}/σ_o distribution beneath the centre line of the component



(b) Normalised residual stress σ_{xx}/σ_o distribution beneath the centre line of a shot

Fig. 2 Numerical validation of two shots impacting on a component

4. Shot impacting with overlap

Following the numerical validation, an extensive parametric study of two/multiple shots impacting normally on a component was conducted. The aim was to investigate systematically the effect of shots impacting with overlap on the residual stress pattern. The numerical results from this study thus gave a sound basis for investigating whole shot peening process by using combined finite element and discrete element analysis (Hong *et al.* 2007).

In the present model, the component is assumed to be a linear elastic strain-hardening plastic material with elastic modulus $E = 200$ GPa, Poisson's ratio $\nu = 0.3$, density $\rho = 7800$ kg/m³ (steel), initial yield stress $\sigma_o = 760$ MPa and linear strain-hardening parameter $H^1 = 500$ MPa. The effect of initial yield stress σ_o and linear strain-hardening parameter H^1 on the residual stress distribution was extensively studied by Hong *et al.* (2005). Identical shots are used in the preset study and the diameter of shot is $d_s = 1$ mm. Using a steel density of 7800 kg/m³, the mass of a shot is 4.085 mg. Normal impact case is considered and the reference impacting velocity of shot is 75 m/s. Frictionless is considered between the shot and component during contact. The first shot impacts on the centre of a component and the successive shot impacts on the previous impacted component in which an existing residual stress distribution was induced by the previous impacts as shown in Fig. 3. The separation distance between the impacting points of the first and second shot is c . The impacting velocity of the first and second shot is v_1 and v_2 . The present paper focus on the resulting residual stresses within a component induced by shot impacts, so the interaction between the

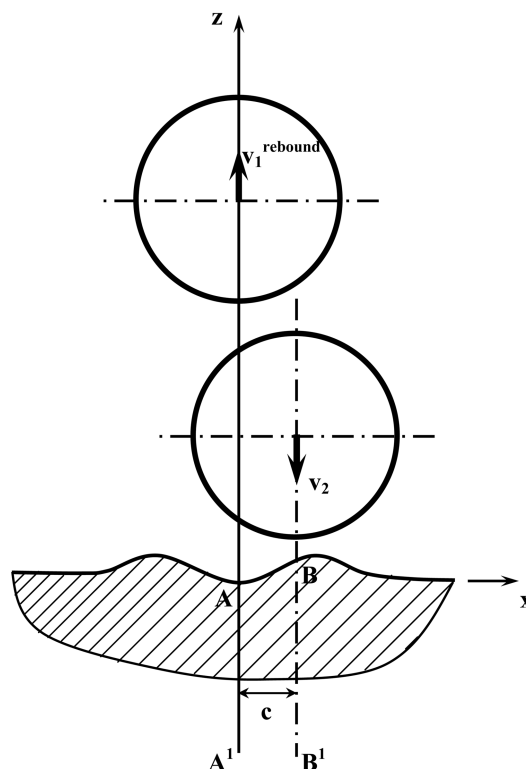


Fig. 3 Shot impacting with overlap

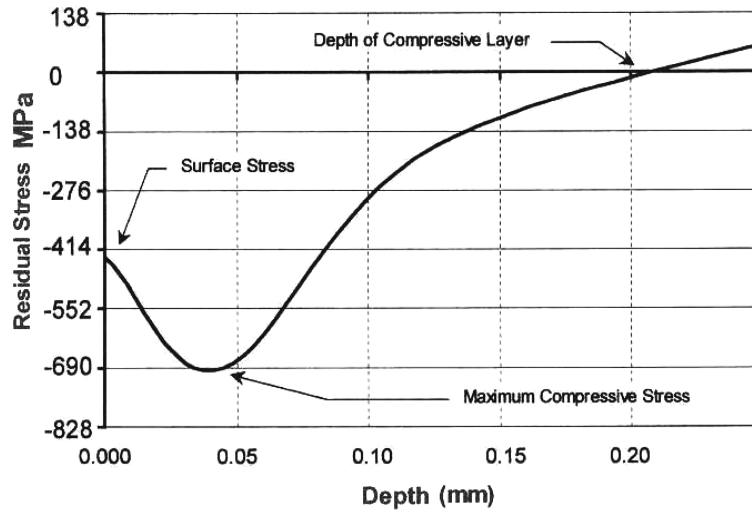


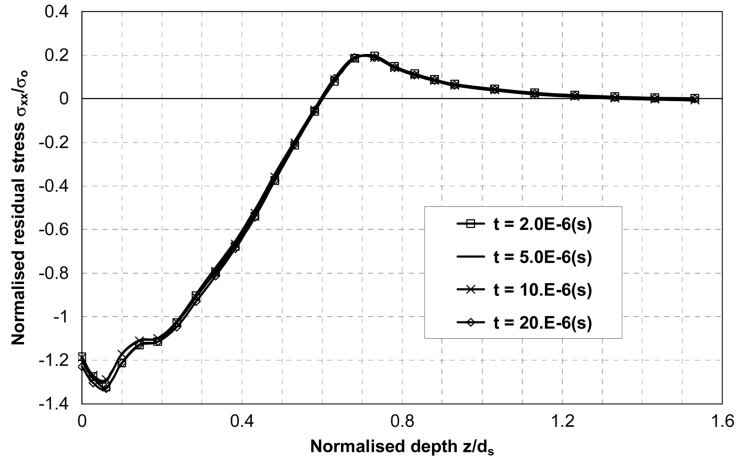
Fig. 4 Typical residual stress profile within a peened component (from MIC 2001)

incoming shot and rebound shot is not considered. Using the discrete element method to simulate a stream of shots delivered onto a component and the interaction between shots was presented in Hong *et al.* (2007).

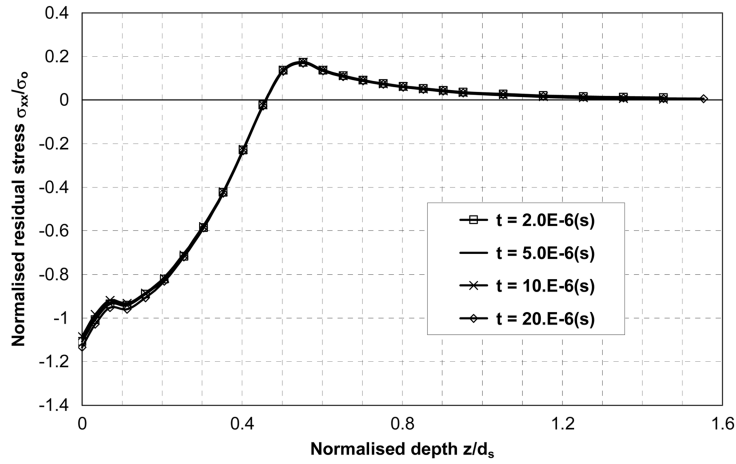
A typical residual stress profile induced by an industrial shot peening process from MIC (2001) is shown in Fig. 4. These stresses are in the planes parallel to the component surface and compressive stresses significantly delay the initiation of fatigue cracking. Three key values that are the most important outcomes from shot peening are highlight in Fig. 4. The first one is the maximum compressive residual stress σ_{\max} , which is the maximum value of the compressive residual stress induced. It is normally just below the component surface. As the magnitude of the maximum compressive residual stress increases so does the resistance to fatigue cracking. The second one is the surface residual stress σ_{surf} , this magnitude is usually less than the maximum compressive residual stress. But for some cases, the maximum residual stress may be predicted at the component surface, not at sub-surface. It means $\sigma_{\max} = \sigma_{\text{surf}}$. The final one is the depth of compressive residual stress layer z_0 , which is the depth of compressive layer resisting crack growth. The results presented in this paper are plotted in a normalised manner using the normalised depth z/d_s , in which z is the deformed depth along the assigned line within a component. In the present study of shots impacting normally on a component, the residual stress component σ_{yy} is same as the component σ_{xx} except for along different coordinate axis. So only the residual stress component σ_{xx} was measured and normalised with σ_0 initial yield stress of the component. All residual stress distributions are plotted with the deformed depth beneath the impacting point of the first shot ($A-A^1$ line in Fig. 3) and the second shot ($B-B^1$ line in Fig. 3) unless otherwise specified.

4.1 Effect of time interval between shot impacts

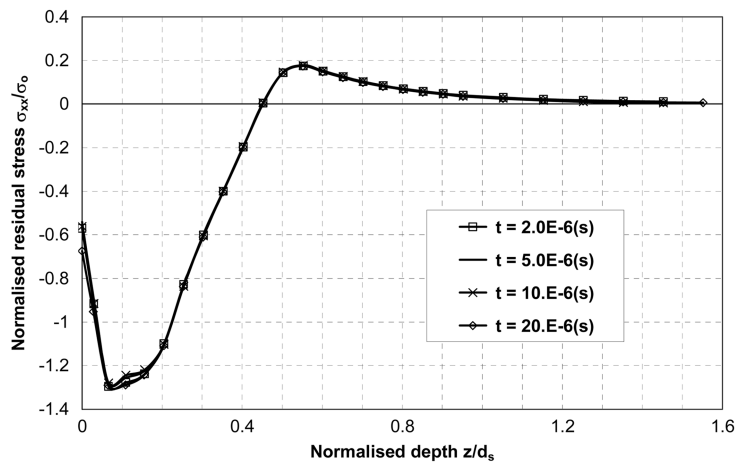
According to the analysis of single shot impacting on a component, it is known that the contact between a shot and the component during the impact is a very short period (less than $10 \mu\text{s}$) (Hong *et al.* 2005). In shot peening process the impacts on a component is always sequential, it can be



(a) Normalised residual stress σ_{xx}/σ_0 distribution along A-A¹ line ($c = 0$)



(b) Normalised residual stress σ_{xx}/σ_0 distribution along A-A¹ line ($c = 0.2d_s$)



(c) Normalised residual stress σ_{xx}/σ_0 distribution along B-B¹ line ($c = 0.2d_s$)

Fig. 5 Effect of time interval between shot impacts

observed in the simulation of whole shot peening process by using discrete element analysis (Hong *et al.* 2007). Meanwhile the time interval between shot impacts is random. So the influence of the time interval between shot impacts on the residual stress profile within a component was investigated. Four different time intervals $t = 2, 5, 10, 20 \mu\text{s}$ were adopted, and the impacting velocity of shots is $v_1 = v_2 = 75 \text{ m/s}$. Two cases with different separation distance $c = 0$ (both shots impacting on point A) and $c = 0.2d_s$ were examined. The automatic time incrementation scheme in ABAQUS/Explicit was used. A stability limit based on the highest element frequency in the whole model was determined using the current dilatational wave speed in each element. In the present study, the time incrementation was about $0.0056 \mu\text{s}$. It took about 3600 time steps for simulating time $t = 20 \mu\text{s}$ and the CPU time was about 4 seconds using Intel Pentium4 (1.9 GHz) Processor.

Figs. 5(a) and 5(b) show the normalised residual stress distributions along $A-A^1$ line after the second shot impact for these two cases of $c = 0$ and $c = 0.2d_s$ respectively. The differences between the normalised results for different interval are extremely small. For the case of $c = 0.2d_s$, the normalised residual stress distribution beneath the impacting point of the second shot ($B-B^1$ line in Fig. 3) is plotted in Fig. 5(c). The difference between the results for different interval is not significant too. The choice of the time interval between the first and second shot impact $t = 10 \mu\text{s}$ used in the following studies was clearly the correct decision.

4.2 Effect of separation distance between the impacting points

The effect of separation distance between the impacting points of the first and second shot on residual stress distribution within a component was investigated with a wide range of separation distance.

First the case of separation distance $c = 0$ was studied. Due to these two shots impact at same point on the component surface, only the residual stress distribution along $A-A^1$ line is plotted. The residual stress distribution created by the second shot impact is compared with that induced by the first shot impact in Fig. 6(a). It can be seen that the magnitudes of the surface residual stress and the maximum compressive residual stress increased slightly as the component is impacted by the second shot. For the depth of the compressive residual stress layer, the impact of the second shot appears to have a significant effect. It increased from $0.43d_s$ to $0.6d_s$ as the second shot impacted.

Then the results with the separation distance $c = d_s$ are shown in Fig. 6(b). In this figure the normalised residual stress distributions along $A-A^1$ line and $B-B^1$ line for two shots impact case are compared with those predicted from single shot impact. The similar residual stress distributions along $A-A^1$ line for both cases show that the successive impact of the second shot does not appear to have any noticeable effect on the existing residual stresses along $A-A^1$ line created by the first shot impact. Due to the residual stresses along $B-B^1$ line induced by the first shot impact are very small, the second shot impacting at point B seems to impact on an un-peened component. So the residual stress distribution along $B-B^1$ line induced by the second shot impact is almost same as that along $A-A^1$ line generated by the first shot impact.

Fig. 7(a) shows the contour of residual stress σ_{xx} within x - z plane ($y = 0$) after the first shot impacting on a component. The contour which is identical for all cases with different separation distances is stated for ease to reference to the residual stress distribution induced by the second shot impact. It shows that the second shot is incoming, and the separation distance between the first and second shot is $0.2d_s$ in this figure. The contour of residual stress σ_{xx} generated by the second shot impacting on a previously impacted component with the separation distance $c = 0.2d_s$ is shown in

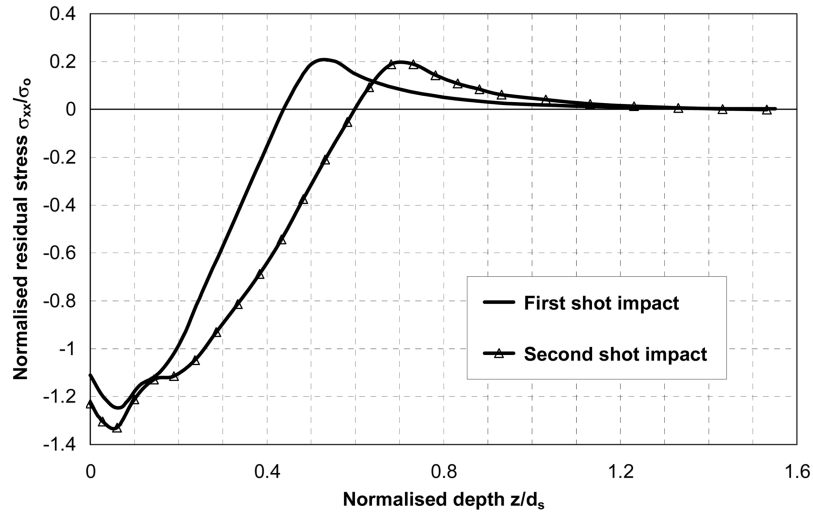
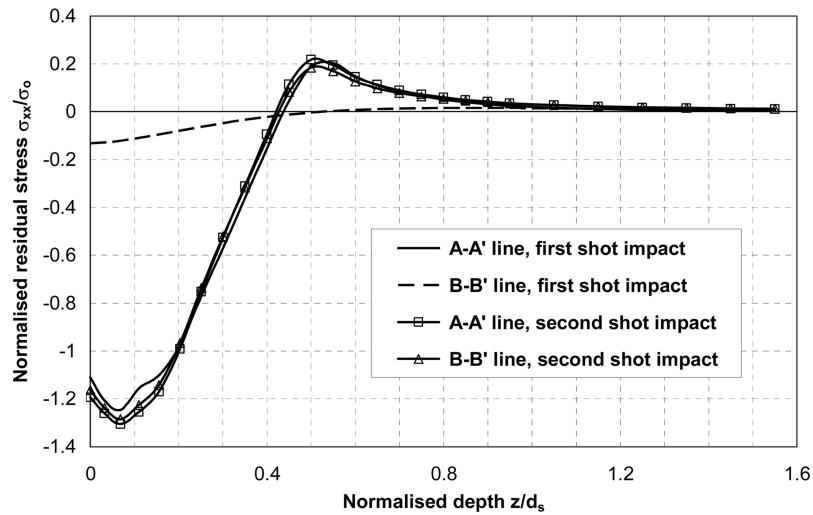
(a) Normalised residual stress σ_{xx}/σ_0 distribution beneath impacting point ($c=0$)(b) Normalised residual stress σ_{xx}/σ_0 distribution ($c = d_s$)

Fig. 6 Effect of separation distance between impacting points

Fig. 7(b). Compared to the residual stress profile before the second shot impact as shown in Fig. 7(a), the difference between these two contours is significant. The maximum compressive residual stress occurs beneath the impacting area of the second shot and the zone with a high residual stress (as $1.2\sigma_0$ in Fig. 7(b)) is enlarged due to the second shot impact. As impacting on a deformed surface, the second shot rebounds with a horizontal velocity v_{2x} which is zero before impacting on the component.

Since the predictions of the surface residual stress, the maximum compressive residual stress and the depth of compressive residual stress layer are the most important outcomes for shot peening analysis, the relationship between these and separation distance c was explored in Figs. 8(a)-(d).

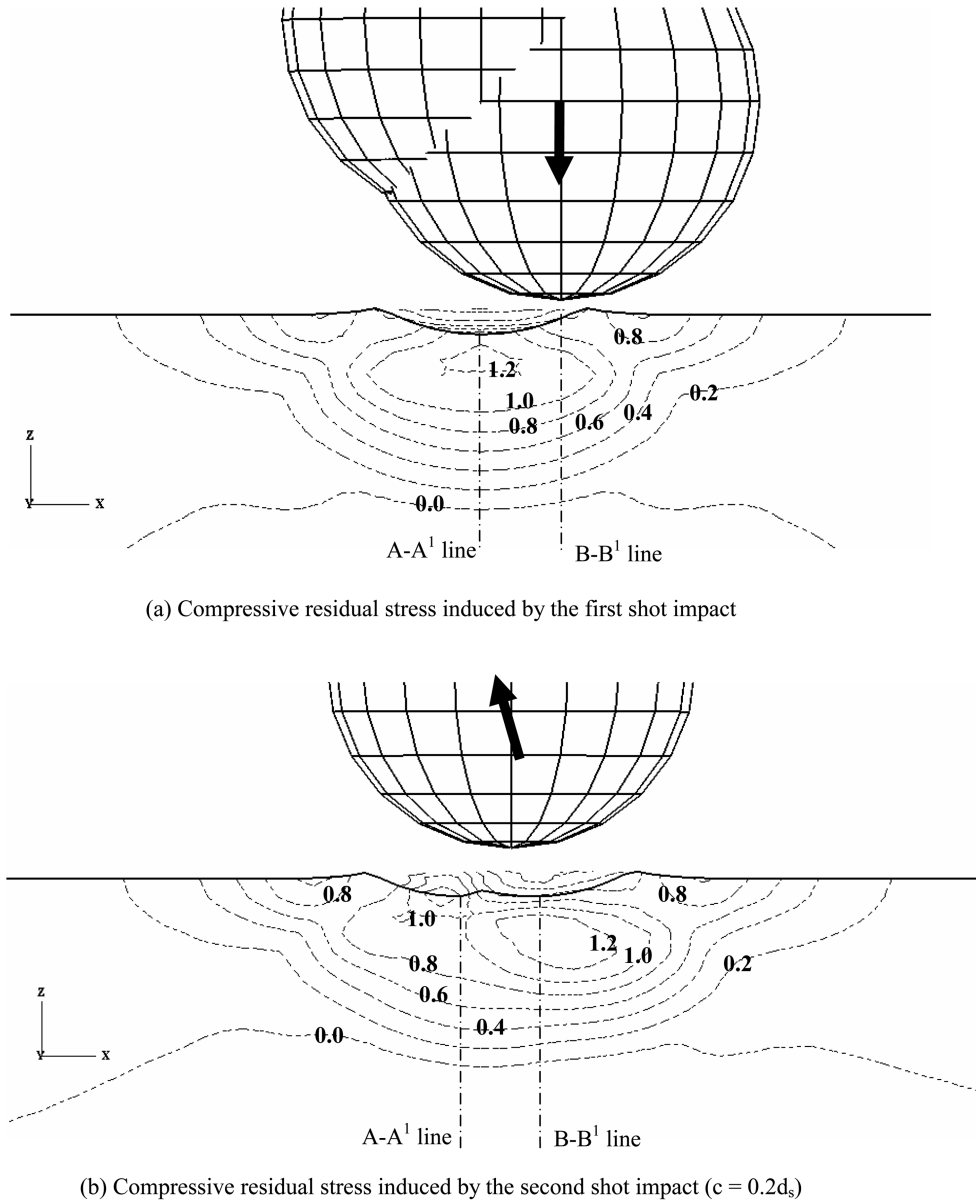
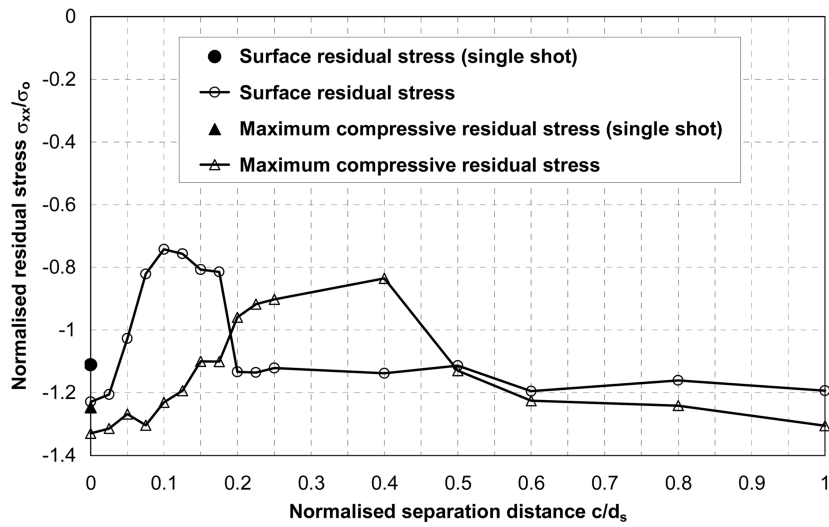


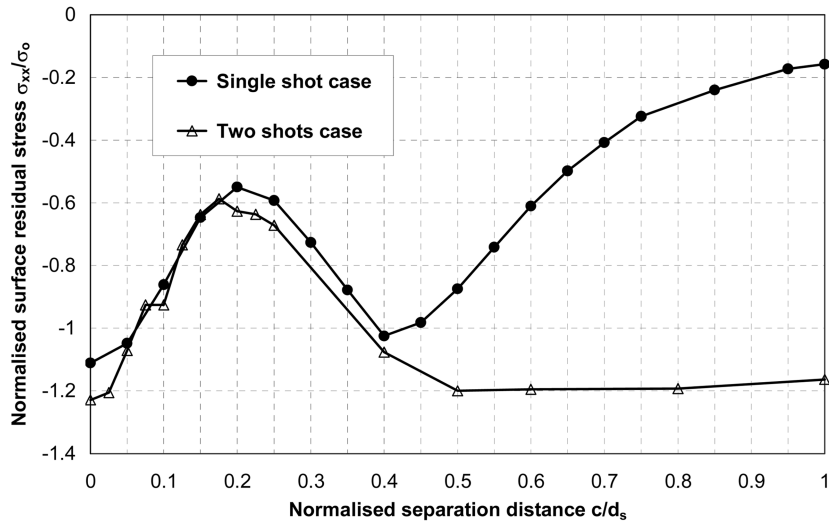
Fig. 7 Contour of normalised compressive residual stress σ_{xx}/σ_0

Firstly, the magnitudes of surface residual stress and maximum compressive residual stress along $A-A'$ line with different separation distances are plotted in Fig. 8(a). The magnitudes of the residual stresses induced by single shot impact are stated for ease to reference, in which the circular spot denotes the surface residual stress at point A and the triangle spot is the magnitude of the maximum compressive residual stress. The effect of the second shot impact on the residual stress profile is significant. When the second shot impacts in the range of $0 \leq c \leq 0.1d_s$, a larger magnitude of the maximum residual stress is obtained by the second shot impact than that of single shot impact, but

this residual stress is decreased with increasing separation distance. Meanwhile, a larger surface residual stress is predicted by the second shot impact only when the second shot impacts in a smaller range, the surface residual stress decreases very quickly from $1.23\sigma_0$ to $0.82\sigma_0$ as the separation distance increases from 0 to $0.1d_s$. When the second shot impacts in the range of $0.1d_s < c \leq 0.175d_s$, the magnitudes of surface residual stress and maximum residual stress induced by the second shot impact are smaller than those of single shot impact. The surface residual stress remains relatively constant and the maximum residual stress decreases with increasing separation distance. The situation of the second shot impacting with partial overlap contact areas ($0.175d_s < c < 0.5d_s$) is considered. In this case, the maximum residual stress along $A-A^1$ line occurs at the component



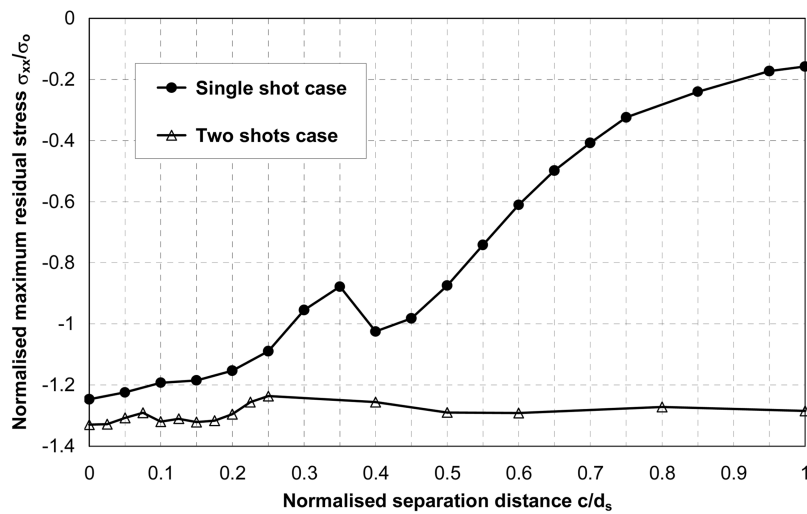
(a) Normalised residual stress along $A-A^1$ line vs. normalised separation distance



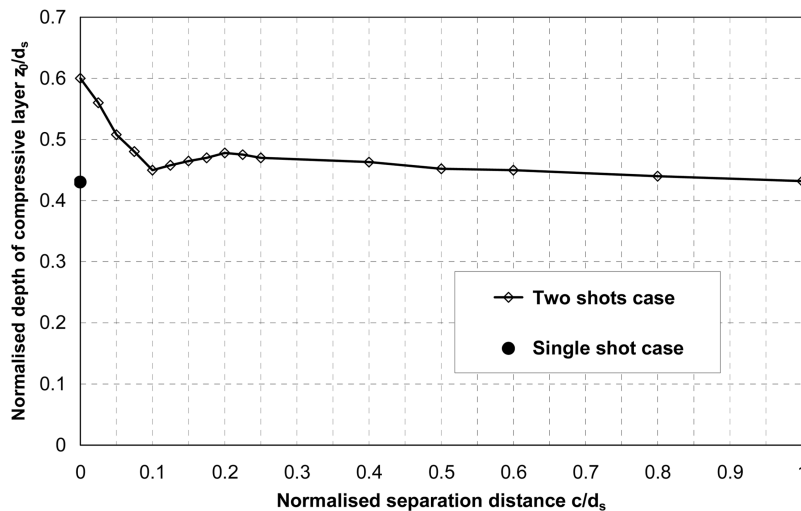
(b) Normalised surface residual stress at point B vs. normalised separation distance

Fig. 8 Effect of separation distance between impacting points

surface (point A) and the magnitude of the residual stress remains almost constant as the surface residual stress of single shot impact. The second shot impact did not appear to have any noticeable effect on the surface residual stress, but showed a significant effect on the sub-surface residual stress. Exactly, the values on the line of maximum residual stress with $c = 0.2d_s, 0.225d_s, 0.25d_s, 0.4d_s$ are the maximum sub-surface residual stress, not the maximum residual stress. Due to the second shot impact, the magnitude of the maximum sub-surface residual stress decreases significantly to a small value. Varying the separation distance in this range, it appears that no significant effect on the surface and maximum sub-surface residual stress. When the second shot impacts with non-overlap contact areas ($0.5d_s \leq c \leq 1.0d_s$), the effect of the second shot impact on



(c) Normalised maximum residual stress on B-B¹ line vs. normalised separation distance



(d) Normalised depth of compressive layer z_0/d_s vs. normalised separation distance

Fig. 8 Continued

the residual stress distribution along $A-A^1$ line is slight, and this effect is decayed with separation distance increasing.

Then the effect of the second shot impact on the residual stress profile along $B-B^1$ line was investigated. The surface residual stress and the maximum residual stress were plotted separately in order to demonstrate clearly. Fig. 8(b) shows the variation of the surface residual stress at point B with separation distance. In this study, the position of point B (impacting point of the second shot) is moved with varying separation distance, the surface residual stress at point B induced by single shot impact with different separation distances was plotted in an attempt to identify the effect of the second shot impact. Two separate phenomena are indicated in Fig. 8(b). When the second shot impacts in the range of $0 \leq c \leq 0.4d_s$, the surface residual stress created by two shots impact remains almost same value as that of single shot impact. It appears that the magnitude of the surface residual stress is mainly determined by the existing residual stress induced by previous impact and the second shot impact has no significant influence on the surface residual stress. On other hand, when the second shot impacts in the range of $0.4d_s < c \leq 1.0d_s$, the effect of the second shot impact on the surface residual stress is significant and the existing residual stress induced by the first shot has no noticeable influence on the residual stress created by successive impact. The magnitude of the surface residual stress after two shots impact remains almost constant at $1.2\sigma_o$ with varying separation distance.

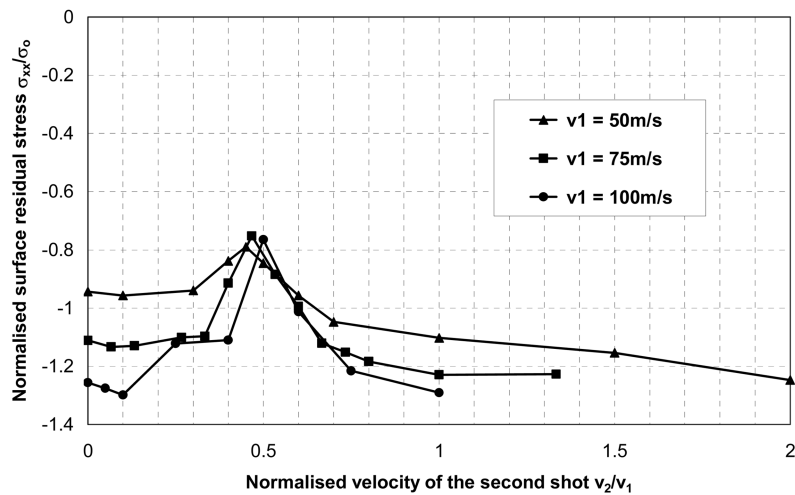
Fig. 8(c) shows the relationship between the maximum compressive residual stress on $B-B^1$ line and separation distance. In single shot impact case, the maximum compressive residual stress on $B-B^1$ line occurs at the component surface when the distance between $B-B^1$ line and the $A-A^1$ line is larger than $0.35d_s$, so the values of the maximum residual stress for $c \geq 0.35d_s$ in this figure are same as the magnitudes of the surface residual stress shown in Fig. 8(b). It can be seen that as the second shot impacts, a larger value of the maximum residual stress is obtained. The magnitude of the maximum residual stress remains relatively constant between $1.23\sigma_o$ to $1.33\sigma_o$, although the existing residual stress induced by the first shot impact varies significantly with different position of $B-B^1$ line. The influence of separation distance on the maximum residual stress created by the second shot impact is less significant than that on the surface residual stress.

The relationship between the depth of compressive residual stress layer and the separation distance was explored in Fig. 8(d). The depth of compressive residual stress layer, which is the maximum depth of whole compressive residual stress zone, is normalised with the shot diameter d_s . It can be seen that the normalised depth of compressive residual stress zone increases from 0.43 to 0.6 due to the second shot impacts at the same point of the first shot. With the separation distance increasing from 0 to $0.1d_s$, the normalised depth of the compressive layer decreases from 0.6 to 0.45 and remains relatively constant between 0.43-0.48 as the separation distance increases further. Although the second shot impact does not generated a deeper layer of compressive residual stress when the separation distance *exceeds* $0.1d_s$, the compressive residual stress zone is enlarged in horizontal direction due to the second shot impact as shown in Fig. 7.

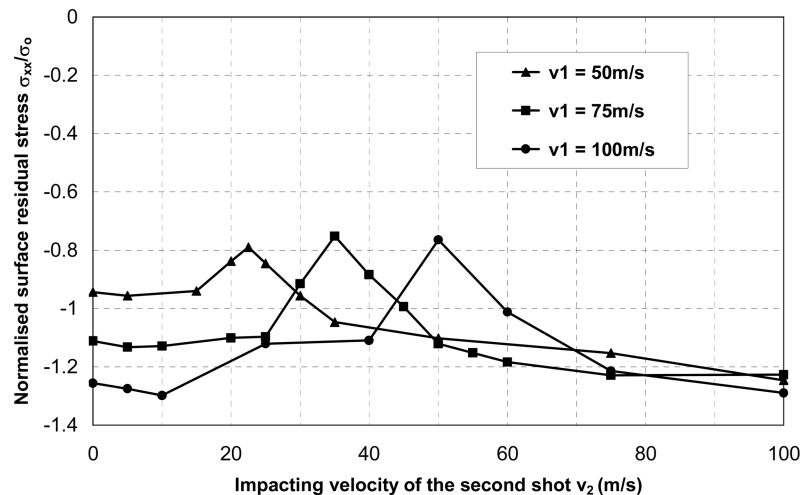
4.3 Effect of impacting velocity of the second shot

The effect of impacting velocity of the second shot was investigated. In this parametric study, three different velocities of the first shot $v_1 = 50, 75, 100$ m/s were adopted and a number of simulations covering a range of impacting velocity of the second shot were performed. The separation distance $c = 0$ was used. Fig. 9(a) shows the relationship between the surface residual

stress at the impacting point and the normalised impacting velocity v_2/v_1 . The surface residual stress with $v_2/v_1 = 0$ is that of single shot impacting on a component. In general, the surface residual stress increases with increasing velocity of the first shot which is agreement the result for single shot impact case. The effect of impacting velocity on the residual stress profile for single shot impacting on a component with different material properties was studied by Hong *et al.* (2005). In Fig. 9(a), it reveals that the surface residual stress is significantly affected by the velocity of the second shot. In general, the surface compressive residual stress decreases with increasing impacting velocity of the second shot when the velocity is small and arrives at a smallest value before increasing as velocity v_2 increases further. It is interesting to note that the surface compressive residual stress drops to the lowest value about $0.8\sigma_o$ when the normalised impacting velocity of the second shot is 0.5 for these three cases with different velocities of the first shot.



(a) Normalised surface residual stress vs. normalised velocity of the second shot



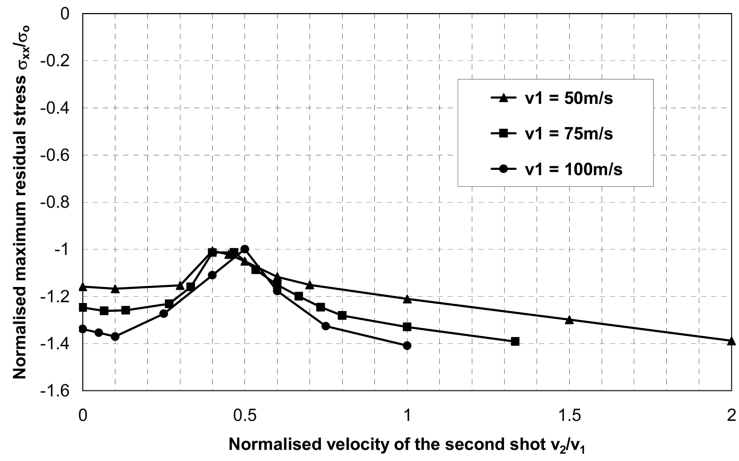
(b) Normalised surface residual stress vs. impacting velocity of the second shot

Fig. 9 Effect of impacting velocity of the second shot ($c = 0$)

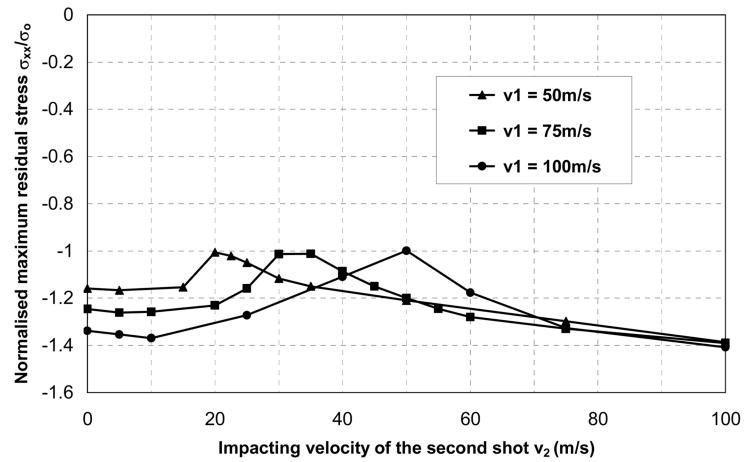
For further clarity, the relationship between the surface residual stress at point A and the velocity of the second shot in Fig. 9(a) is re-plotted in Fig. 9(b) with the direct value of the impacting velocity of the second shot in m/s. The practical range of impacting velocity in industrial shot peening is 25-100 m/s. The results for the low velocity (less than 25 m/s) are shown in the figure in order to understand the behaviour of the successive impact. It is clear from the results shown in Fig. 9(b) that the second shot impact is beneficial for creating a compressive residual stress as the magnitude of the surface residual stress increases from $0.95\sigma_o$ to $1.25\sigma_o$ with the velocity v_2 increasing from 30 m/s to 100 m/s if the velocity of the first shot v_1 is 50 m/s. For this case, the surface residual stress induced by the first shot is about $0.95\sigma_o$. For the case of impacting velocity of the first shot $v_1 = 75$ m/s, the effect of the second shot impact on the surface residual stress is strongly depended on impacting velocity of the second shot v_2 and $v_2 = 50$ m/s is the key point. When the velocity v_2 is in the range of 25 m/s-50 m/s, the compressive surface residual stress induced by the second shot impact is always smaller than that of the first shot impact. And the smallest value of the surface residual stress created by the second shot impact is only $0.75\sigma_o$ occurring with $v_2 = 35$ m/s, which is significantly smaller than that of the first shot impact $\sigma_{surf} = 1.1\sigma_o$. On other hand, when the velocity v_2 exceeds 50 m/s, the resulting residual stress induced by the second shot impact is slightly increasing from $1.1\sigma_o$ to $1.23\sigma_o$ as the velocity v_2 increases from 50 m/s to 100 m/s. When the first shot with the highest velocity $v_1 = 100$ m/s impacting on the component, a high compressive surface residual stress (about $1.25\sigma_o$) is generated at the impacting point. This residual stress is decreased as the second shot impacting if the impacting velocity of the second shot is smaller than 100 m/s. The magnitude of the smallest surface residual stress is about $0.78\sigma_o$ occurring with $v_2 = 50$ m/s. So the effect of the second shot impact on the existing surface residual stress is negative unless the velocity of the second shot is not less 100 m/s. Comparing the magnitudes of the surface residual stress occurring with $v_2 = 75, 100$ m/s in Fig. 9(b), it can be seen that the differences along these three cases with different velocities v_1 are very small. This is in contrast with the results occurring with a smaller velocity of the second shot where significant differences can be seen along the cases with different velocities v_1 . It appears that the surface residual stress is mainly determined by the impacting velocity of the second shot when this velocity v_2 is relatively high (≥ 75 m/s for this study). In other words, when the velocity v_2 is not sufficiently high, the surface residual stress depends not only on the velocity of the second shot v_2 , but also on the existing residual stresses within the previously impacted component.

Then, Fig. 10(a) shows the relationship between the maximum compressive residual stress along $A-A^1$ line and the normalised velocity of the second shot v_2/v_1 . Although the effect of the impacting velocity of the second shot v_2 on the maximum residual stress was less significant than that on the surface residual stress, it can be seen that the effect on both the maximum and surface residual stress is in similar fashion. The smallest magnitude of the maximum residual stress induced by the second shot impact occurs with the velocity $v_2 \approx 0.5v_1$ for all three cases of different velocity $v_1 = 50, 75, 100$ m/s. Also, the smallest value of the residual stress is almost same and equals to initial yield stress of the component σ_o . Again, the relationship between the maximum residual stress and the velocity of the second shot is re-plotted in Fig. 10(b) with the direct value of the impacting velocity v_2 in m/s. Similar phenomena can be seen.

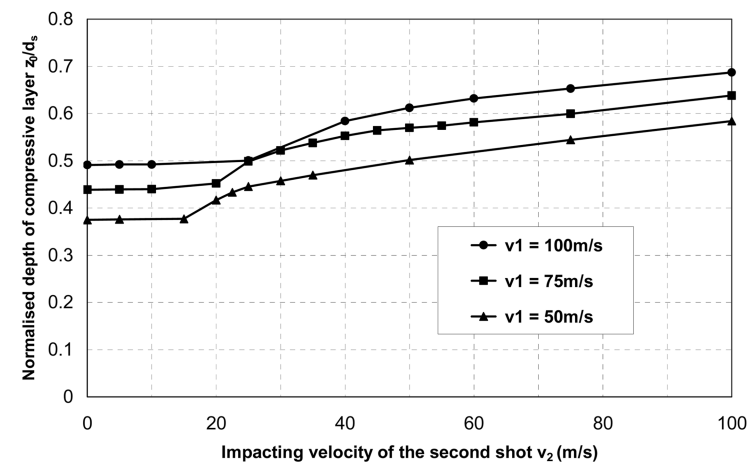
Finally, the variation of the depth of compressive residual stress layer with the impacting velocity of the second shot is shown in Fig. 10(c). It is clear that the second shot impact is beneficial for extending the compressive residual stress zone deeply within the component. For the case of $v_1 = 50$ m/s, the depth increases linear with the velocity of the second shot v_2 increasing from 25 m/s to



(a) Normalised maximum residual stress vs. normalised velocity of the second shot



(b) Normalised maximum compressive residual stress vs. velocity of the second shot



(c) Normalised depth of compressive layer z_0/d_s vs. impacting velocity of the second shot

Fig. 10 Effect of impacting velocity of the second shot ($c = 0$)

100 m/s. Since the second shot impacting, the depth increases from $0.37d_s$ created by the first shot impact to $0.58d_s$ when the velocity v_2 is 100 m/s. In the case of $v_1 = 100$ m/s, the depth of compressive residual stress layer remains almost same as that induced by the first shot impact when the velocity of the second shot v_2 is only 25 m/s. Then the depth increases from $0.5d_s$ to $0.68d_s$ with the velocity v_2 increasing from 25 m/s to 100 m/s, and the relationship between the depth and the velocity v_2 is linear when $v_2 > 60$ m/s. Also, the effect of impacting velocity of the first shot on the depth of compressive residual stress layer is significant. When the velocity v_2 is not less than 60 m/s, the depth of compressive residual stress layer increases linearly with the velocity of the first shot v_1 .

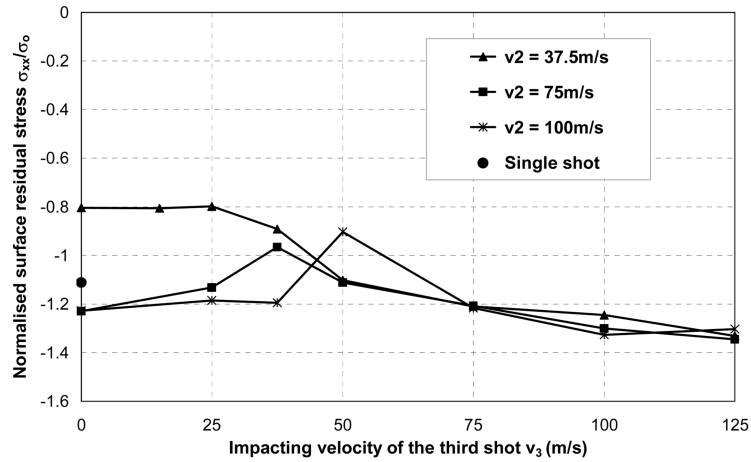
In this study, an interesting finding is that a residual stress relaxation may occur with the second shot impact, depending on the velocity of the second shot with respect to that of the first shot. The residual stress relaxation is related to the magnitude of the residual stress. The surface residual stress decreases from the value induced by the first shot impact to about $0.8\sigma_o$ whereas the maximum residual stress decreasing to about $1.0\sigma_o$ when the ratio of the velocity v_2/v_1 is 0.5. The main conclusion is therefore that the magnitude of the surface residual stress is strongly influenced by the impacting velocity of the second shot and the depth of compressive residual stress layer increases with increasing velocity of the second shot. Comparing the effect of the second shot impact on the maximum residual stress with that on the surface residual stress, the effect on the maximum residual stress is relatively small.

4.4 Effect of impacting velocity of the third shot

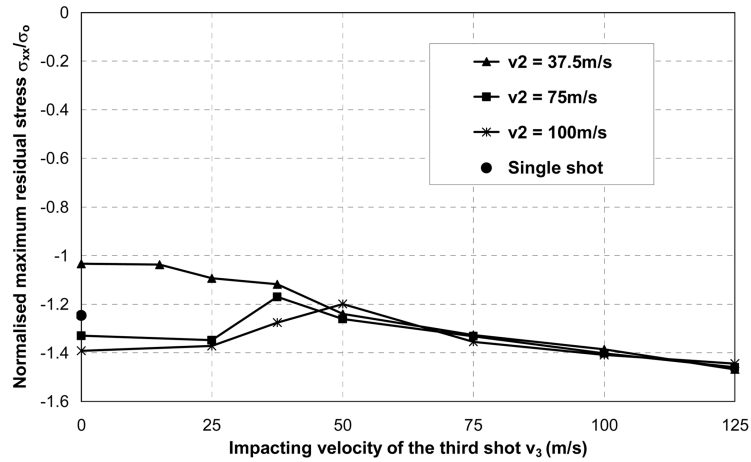
A further study of the effect of shot impacting with overlap on the residual stress profile within a component was conducted by investigating three shots impacting normally on a component. In this study, three shots impact successively at the same point on the component surface, so the separation distance along the impacting points of these three shots is $c = 0$. The second and third shot impacts on a previously impacted area in which an existing residual stress distribution was induced by previous shot impacts. The impacting velocity of the first shot v_1 is 75 m/s and three different impacting velocities of the second shot $v_2 = 37.5, 75, 100$ m/s were adopted for three different case studies. A number of simulations covering a range of impacting velocities of the third shot were performed.

The relationship between the surface residual stress, the maximum compressive residual stress, the depth of compressive residual stress layer and the impacting velocity of the third shot was explored in Figs. 11(a)-(c). In these figures, the circular spot denotes the value for the case of single shot impact and the values at $v_3 = 0$ are predicted from the case of two shots impacting on a component as described above.

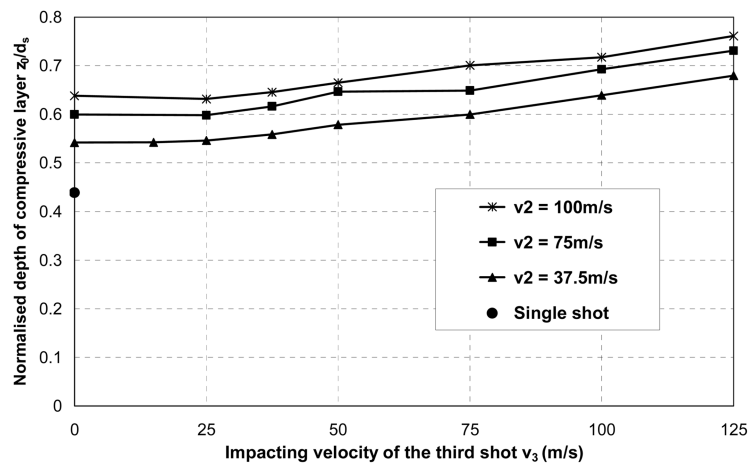
The variation of the normalised surface residual stress at the impacting point (point A) as a function of the velocity of the third shot is shown in Fig. 11(a). As mentioned above, the practical range of impacting velocity in industrial shot peening is 25-100 m/s. In an attempt to clarify the effect of successive shot impact, the results for the velocity lying outside the practical range are still shown in the figure. It is clear from the results that the residual stress relaxation may occur with $v_2 = 75$ m/s and 100 m/s. In the case of $v_2 = 75$ m/s, the surface residual stress decreases from $1.23\sigma_o$ (the residual stress before the third shot impact) to $0.96\sigma_o$ as the third shot impacting with velocity $v_3 = 37.5$ m/s, whereas for the case of $v_2 = 100$ m/s, the surface residual stress decreases from $1.22\sigma_o$ to $0.9\sigma_o$ as the third shot impacting with $v_3 = 50$ m/s. For the case of $v_2 = 37.5$ m/s, the resulting surface residual stress is strongly influenced by the velocity of the third shot, it increases



(a) Normalised surface residual stress vs. impacting velocity of the third shot



(b) Normalised maximum compressive residual stress vs. impacting velocity of the third shot



(c) Normalised depth of compressive layer z_0/d_s vs. impacting velocity of the third shot

Fig. 11 Effect of impacting velocity of the third shot ($c = 0$)

from $0.8\sigma_o$ to $1.25\sigma_o$ with the velocity v_3 increasing from 25 m/s to 100 m/s. No residual stress relaxation occurs with the third shot impact in this case. It is noted that the magnitudes of the surface residual stress are nearly same for these three cases with different velocity of the second shot, when the velocity of the third shot is high (≥ 75 m/s). Furthermore, the differences between the results for $v_2 = 37.5$ m/s and $v_2 = 75$ m/s are extremely small when the velocity $v_3 \geq 50$ m/s.

The relationship between the maximum compressive residual stress along $A-A^1$ line and the velocity of the third shot is shown in Fig. 11(b). The effect of the velocity of the third shot on the magnitude of maximum residual stress is not as pronounced as that on the magnitude of surface residual stress. The magnitude of the maximum residual stress decreases slightly due to the third shot impact if the velocity v_3 lies in the range of 25 m/s-75 m/s for the cases of $v_2 = 75$ m/s and 100 m/s. This is in contrast with the case of the smallest velocity $v_2 = 37.5$ m/s where the residual stress has a significant increasing as the third shot impact. Also it can be seen that the maximum residual stresses of these three cases with different velocity v_2 are almost same when the velocity of the third shot is higher than 37.5 m/s. It reveals that the resulting residual stresses induced by the third shot impact are mainly determined by the impacting velocity of the third shot when this velocity is sufficient high. This is a similar fashion that has been observed in the case of two shots impact on a component.

Finally, the relationship between the depth of compressive residual stress layer and the velocity of the third shot is shown in Fig. 11(c). It is clear that the depth of compressive residual stress layer increases with increasing the velocity of the third shot for these cases of different velocity $v_2 = 37.5, 75, 100$ m/s. Apparently, the impact of successive shots causes a deeper compressive residual stress layer, such as the depth of the first shot impact is $0.43d_s$, then increased to $0.65d_s$, as the successive shots impact ($v_2 = v_3 = 75$ m/s).

6. Conclusions

A three-dimensional dynamic finite element analysis of two/multiple shots impacting on a metallic component has been presented. The model was validated against another published numerical study. An extensive parametric study has been conducted to investigate the effect of shot impacting with overlap on the residual stress distribution. The parameters investigated include time interval between shot impacts, separation distance between the impacting points, and impacting velocity of the successive shots.

The impact of successive shots has a significant effect on the existing residual stress distribution within the component induced by previous shot impacts. An interesting finding is that a residual stress relaxation may occur with the successive impacts. The reduction of the residual stress is mainly determined by the ratio of velocity of the successive and previous shot. However the depth of the compressive residual stress layer always increases as the successive shot impacts.

The present numerical study demonstrated the behaviour of shot impacting with overlap and characterised the effect of multiple, overlapping impacts. The present results should be useful for studying the effects of repeated impacts, impacting sequence and peening coverage on the residual stress profile.

Acknowledgements

The authors gratefully acknowledge the funding for this work from the UK Engineering and Physical Sciences Research Council (EPSRC Grant, GR/R28188), with contributions from ISPC Impact Finishers.

References

- ABAQUS. (2002), *Theory and Users Manual*, Version 6.3, Pawtucket, Rhode Island, Habbitt, Karlsson and Sorensen Inc.
- Al-Hassani, S.T.S. (1981), "Mechanical aspects of residual stress development in shot peening", *Proc. ICSP-1*, Paris, 583-602.
- Al-Hassani, S.T.S., Kormi, K. and Webb, D.C. (1999), "Numerical simulation of multiple shot impact", *Proc. of ICSP-7*, Warsaw, Poland, 217-227.
- Baragetti, S. (2001), "Three-dimensional finite element procedures for shot peening residual stress field prediction", *Int. J. Comput. Appl. Technol.*, **14**, 51-63.
- Deslaef, D., Rouhaud, E. and Rasouli-Yazdi, S. (2000), "3D finite element models of shot peening processes", *Mater. Sci. Forum.*, **347-349**, 241-246.
- Edberg, J., Lindgren, L. and Mori, K. (1995), "Shot peening simulated by two different finite element formulations", In: Shen, Dawson, editors. *Simulation of Materials Processing: Theory, Methods and Applications -NUMIFORM95*, 425-430.
- Goldsmith, W. (1960), *Impact the Theory and Physical Behaviour of Colliding Solids*, London, Edward Arnold.
- Guagliano, M., Vergani, L., Bandini, M. and Gili, F. (1999), "An approach to relate the shot peening parameters to the induced residual stresses", *Proc. of ICSP-7*, Warsaw, Poland, 274-282.
- Hardy, C., Baronet, C.N. and Tordion, G.V. (1971), "The elasto-plastic indentation of a half-space by a rigid sphere", *Int. J. Numer. Meth. Eng.*, **3**, 451-462.
- Hertz, H. (1882), "Uber die Beruhrung fester elastischer Korper (On the contact of elastic solids)", *J. Reine Angewandte Mathematik*, **92**, 156-171.
- Hills, D.A., Waterhouse, R.B. and Noble, B. (1983), "An analysis of shot peening", *J. Strain Analysis*, **18**, 95-100.
- Hong, T., Ooi, J.Y. and Shaw, B.A. (2005), "Three-dimensional finite element analysis of residual stress induced by single/multiple shots impact", *Internal Report*, School of Engineering & Electronics, University of Edinburgh.
- Hong, T., Ooi, J.Y. and Shaw, B.A. (2007), "A numerical simulation to relate the shot peening parameters to the induced residual stresses", Submitted to *International Journal of Fatigue*.
- Johnson, W. (1972), *Impact Strength of Materials*, London, Edward Arnold.
- l-Obaid, Y.F. (1995), "Shot peening mechanics: Experimental and theoretical analysis", *Mech. Mater.*, **19**, 251-260.
- Meguid, S.A., Shagal, G. and Stranart, J.C. (2002), "3D FE analysis of peening of strain-rate sensitive materials using multiple impingement model", *Int. J. Impact Eng.*, **27**, 119-134.
- Meguid, S.A., Shagal, G., Stranart, J.C. and Daly, J. (1999), "Three-dimensional dynamic finite element analysis of shot-peening induced residual stresses", *Finite Elem. Anal. D.*, **31**, 179-191.
- MIC (2001), *Shot Peening Application*, Eighth edition, Metal Improvement Company, Inc.
- Rouhaud, E. and Deslaef, D. (2002), "Influence of shots' material on shot peening, a finite element model", *Mater. Sci. Forum*, **404-407**, 153-158.
- Schiffner, K. and Helling, C.D. (1999), "Simulation of residual stresses by shot peening", *Comput. Struct.*, **72**, 329-340.